Theoretical uncertainties of the elastic nucleon-deuteron scattering observables

R. Skibiński, Yu. Volkotrub, J. Golak, K. Topolnicki, and H. Witała
M. Smoluchowski Institute of Physics, Jagiellonian University, PL-30348 Kraków, Poland

(Received 29 March 2018; published 2 July 2018)

Theoretical uncertainties of various types are discussed for the nucleon-deuteron elastic scattering observables at incoming-nucleon laboratory energies up to 200 MeV. We are especially interested in the statistical errors arising from uncertainties of parameters of a nucleon-nucleon interaction. The obtained uncertainties of the differential cross section and numerous scattering observables are in general small, grow with the reaction energy, and amount up to a few percent at 200 MeV. We compare these uncertainties with the other types of theoretical errors like truncation errors, numerical uncertainties, and uncertainties arising from using the various models of nuclear interaction. We find the latter ones to be dominant source of uncertainties of modern predictions for the three-nucleon scattering observables. To perform above mentioned studies we use the One-Pion-Exchange Gaussian potential derived by the Granada group, for which the covariance matrix of its parameters is known, and solve the Faddeev equation for the nucleon-deuteron elastic scattering. Thus besides studying theoretical uncertainties we also show a description of the nucleon-deuteron elastic scattering data by the One-Pion-Exchange Gaussian model and compare it with results obtained with other nucleon-nucleon potentials, including chiral N^4LO forces from the Bochum-Bonn and Moscow(Idaho)-Salamanca groups. In this way we confirm the usefulness and high quality of the One-Pion-Exchange Gaussian force.

DOI: 10.1103/PhysRevC.98.014001

I. INTRODUCTION

One of the main goals of nuclear physics is to establish the properties of nuclear interactions. After many years of investigations we are now in a position to study details of nuclear forces both from the theoretical as well as the experimental sides. It has been found that the three-nucleon ($3N$) system, which allows one to probe also the off-energy-shell properties of the nuclear potential, is especially important for such studies. Moreover, to obtain a precise description of the $3N$ data one has to supplement the two-nucleon ($2N$) interaction by a $3N$ force acting in this system. Currently the structure of $3N$ force is still unclear and many efforts are directed to fix $3N$ force properties. However, in order to obtain trustable and precise information from a comparison of $3N$ data with predictions based on theoretical models it is necessary to take into account, or at least to estimate, in addition to the uncertainties of data also the errors of theoretical predictions.

The precision of the experimental data has significantly increased, and has achieved in recent measurements a high level; see, e.g., Refs. [1–5] for examples of state-of-the-art experimental studies in the three-nucleon sector. Precision of these and other experiments has become so high that the question about the uncertainties of the theoretical predictions is very timely [6]. In the past the theoretical uncertainties for observables in three-nucleon reactions were estimated by comparing predictions based on various models of nuclear interactions [7] or by performing benchmark calculations using the same interaction but various theoretical approaches [8–12]. Such a strategy was dictated by (a) a common belief that a poor knowledge about the nuclear forces, reflected by the existence of very different models of nuclear interaction, is a dominant source of the theoretical uncertainty; (b) lack of knowledge about the correlations between nucleon-nucleon (NN) potential parameters; (c) using inconsistent models of $2N$ and $3N$ forces; and last but not least (d) a magnitude of uncertainties of experimental data available at the time. Nowadays these arguments, at least partially, are no longer valid due to the above mentioned progress in experimental techniques, progress in the derivation of consistent $2N$ and $3N$ interactions, e.g., within the chiral effective field theory (χEFT) [13–17], and due to availability of new models of nuclear forces, where free parameters are fixing by performing a careful statistical analysis [18,19]. As a consequence, the estimation of theoretical uncertainties has become again an important issue in theoretical studies.

An extensive introduction to an error estimation for theoretical models was given in Ref. [20], followed by a special issue of *Journal of Physics G: Nuclear and Particle Physics* [21]. In the latter reference many applications of the error estimation to nuclear systems and processes are discussed. However, omitting the few-nucleon reactions, the authors focus mainly on models used in direct fitting to data or on models used in nuclear structure studies. Among the other papers focused on the estimation of theoretical uncertainties of NN interaction we refer the reader to works by Ekström *et al.* [22], Navarro Pérez *et al.* [19,23,24], and to a recent work by Reinert *et al.* [25]. Simultaneously, the Bayesian approach to estimate uncertainties in the $2N$ system was derived in Ref. [26] with some applications shown again in Ref. [21]. Beyond the $2N$ system, the uncertainty of theoretical models has been recently studied in the context of nuclear structure calculations, for which such an evaluation is important also from a practical point of view. Namely, predictions for many-nucleon systems require not only a huge amount of advanced computations

but also rely, e.g., in the case of the no-core shell model [27], on extrapolations to large model spaces. A knowledge of precision of the theoretical models is important for efficient use of available computer resources.

Studies of theoretical uncertainties in few-nucleon reactions are less advanced. Besides the above mentioned attempts to estimate their magnitudes by means of benchmark calculations, most efforts in the field were orientated to estimate uncertainties present in the χEFT approach [13]. In this case three sources of theoretical uncertainties have been investigated: the truncation of the chiral expansion at a finite order (which results in the so-called truncation errors), the introduction of regulator functions (which results in a cutoff dependence), and the procedure of fixing values of low-energy constants. A simple prescription of how to estimate the truncation errors was proposed by Epelbaum and collaborators for the $2N$ system [28] and adopted also for $3N$ systems, for the case where predictions were based on a two-body interaction [29] only. It was found that both for pure nuclear systems [29] as well as for electroweak processes [30] the magnitude of truncation errors strongly decreases with the order of chiral expansion, and at the fifth order (N^{4}LO) it becomes relatively small. The prescription of Ref. [28] is in agreement with the Bayesian approach [26]; see also the recent work [31] for a discussion of the Bayesian truncation errors for the NN observables. The dependence of the chiral predictions on used regulator functions and their parameters has been studied since the first applications of chiral potentials to the $2N$ and $3N$ systems [32–34]. The regulator dependence of chiral forces was broadly discussed in the past (see, e.g., [35]) and various regulator functions were proposed. The nonlocal regularization in the momentum space was initially used and estimations of the theoretical uncertainties of the $2N$ and many-body observables related to regulators were made by comparing predictions obtained with various values of regularization parameters. It was found that the nonlocal regularization leads to an unwanted dependence of observables on the parameters used. This dependence was especially strong for predictions for the nucleon-deuteron (Nd) elastic scattering based on $2N$ and $3N$ forces at the next-to-next-to-next-to leading order (N^{3}LO) of chiral expansion [36] and for the electromagnetic processes in the $3N$ systems when also the leading meson-exchange currents were taken into account [37,38]. These results were one of the reasons for introducing another method, the so-called semilocal method of regularization of chiral forces. Such an improved method was presented and applied to the NN system in Refs. [28,39], leading to weak cutoff dependence of predictions in two-body system at chiral orders above the leading order. A similar picture of weak dependence of predictions based on the chiral forces of Refs. [28,39] was found for Nd elastic scattering [29] and for various electroweak processes [30]. Also the nuclear structure calculations confirmed this observation [40,41].

The estimation of the theoretical uncertainties arising from an uncertainty of the potential parameters (which we will call in the following also a statistical error) has not been studied yet, to the best of our knowledge, in Nd scattering. Within this paper we investigate how such statistical uncertainties propagate from the NN potential parameters to the Nd scattering observables. We also compare them with the remaining theoretical uncertainties for the same observables. To this end we use, for the first time in Nd scattering, the One-Pion-Exchange (OPE) Gaussian NN interaction derived recently by the Granada group [19]. Knowledge of the covariance matrix of the OPE-Gaussian potential parameters is a distinguishing feature of this interaction. This is also crucial for our investigations as we use a statistical approach to estimate theoretical uncertainties. Namely, given the covariance matrix for the potential parameters, we sample 50 sets of the potential parameters and, after calculating for each set the $3N$ observables, we study statistical properties of the obtained predictions. The OPE-Gaussian interaction is described briefly in Sec. II and our method to obtain statistical errors is discussed step by step in Sec. III. The OPE-Gaussian force has been already used, within the same method, to estimate the statistical uncertainty of the ^{3}H binding energy [42], which was found to be around 15 keV ($\approx$0.16%).

The paper is organized as follows: in Sec. II we show the essential elements of our formalism, describe its numerical realization and give some more information on the OPE-Gaussian potential and the chiral models used. In Sec. III we present predictions for the Nd elastic scattering observables obtained with the OPE-Gaussian force and compare them with predictions based on the AV18 NN potential [43]. We also discuss various estimators of uncertainties in hand for the $3N$ scattering observables. In Sec. IV we compare, for a few chosen observables, the theoretical uncertainties arising from various sources, including the truncation errors and the regulator dependence. Here, beside the OPE-Gaussian potential and other semiphenomenological NN forces, we also use the chiral interaction of Ref. [28,39] and, for the first time in Nd scattering, the chiral N^{4}LO interaction recently derived by the Moscow(Idaho)-Salamanca group [17]. Finally, we summarize in Sec. V.

II. FORMALISM

The formalism of the momentum space Faddeev equation is one of the standard techniques to investigate $3N$ reactions and has been described in detail many times; see, e.g., [44,45]. Thus we only briefly remind the reader of its key elements.

For a given NN interaction V we solve the Lippmann-Schwinger equation $t = V + V\tilde{G}_0 t$ to obtain matrix elements of the $2N$ t operator, with $\tilde{G}_0$ being the $2N$ free propagator. These matrix elements enter the $3N$ Faddeev scattering equation which, neglecting the $3N$ force, takes the following form:

$$T|\phi\rangle = tP|\phi\rangle + tPG_0T|\phi\rangle. \tag{2.1}$$

The initial state $|\phi\rangle$ is composed of a deuteron and a momentum eigenstate of the projectile nucleon; G_0 is the free $3N$ propagator and P is a permutation operator.

The transition amplitude for the elastic Nd scattering process $\langle\phi'|U|\phi\rangle$ contains the final channel state $|\phi'\rangle$ and is obtained as

$$\langle\phi'|U|\phi\rangle = \langle\phi'|PG_0^{-1}|\phi\rangle + \langle\phi'|PT|\phi\rangle, \tag{2.2}$$

from which observables can be obtained in the standard way [44].

Equation (2.1) is solved in the partial wave basis comprising all $3N$ states with the two-body subsystem total angular momentum $j \leqslant 5$ and the total $3N$ angular momentum $J \leqslant \frac{25}{2}$.

Since we obtained the bulk of our results with the OPE-Gaussian interaction [19], we now briefly remind the reader of the structure of this potential. A basic concept at the heart of this force is analogous to the one stated behind the well-known AV18 interaction [43]. The OPE-Gaussian potential $V(\vec{r})$ is composed of the long-range $V_{\rm long}(\vec{r})$ and the short-range $V_{\rm short}(\vec{r})$ parts,

$$V(\vec{r}) = V_{\rm short}(\vec{r})\theta(r_c - r) + V_{\rm long}(\vec{r})\theta(r - r_c), \qquad (2.3)$$

where $r_c = 3$ fm and the $V_{\rm long}(\vec{r})$ part contains the OPE force and the electromagnetic corrections. The $V_{\rm short}(\vec{r})$ component is built from 18 operators $\hat{O}_n$, among which 16 are the same as in the AV18 model. Each of them is multiplied by a linear combination of the Gaussian functions $F_k(r) = \exp(-r^2/(2a_k^2))$, with $a_k = \frac{a}{1+k}$, and the strength coefficients $V_{k,n}$:

$$V_{\rm short}(\vec{r}) = \sum_{n=1}^{18} \hat{O}_n \left[\sum_{k=1}^{4} V_{k,n} F_k(r) \right]. \qquad (2.4)$$

The free parameter a present in the $F_k(r)$ functions together with the parameters $V_{k,n}$ have been fixed from the data. It is worth noting that to this end the "3σ self-consistent database" [18] was used. It incorporates 6713 proton-proton and neutron-proton data, gathered within the years 1950 to 2013, in the laboratory energy range $E_{\rm lab}$ up to 350 MeV. The careful statistical revision of data and the fitting procedure allowed the authors of Ref. [19] to confirm good statistical properties of their χ^2 fit, e.g., by checking the normality of residuals. The χ^2/data for the OPE-Gaussian force is 1.06 as fitted to data enumerated in Ref. [18]. We have been provided by the authors of Ref. [19] with 50 sets of parameters $\{V_{k,n}, a\}$ obtained by a correlated sampling from the multivariate normal distribution with a known covariance matrix (see [46] for details). The OPE-Gaussian model, having a similar structure to the AV18 force but being fitted to the newer data, can be regarded as a refreshed version of the standard AV18 model. In the NN sector these two potentials lead to a slightly different description of phase shifts, especially at energies above 150 MeV in the $^3F_2$ and $^3D_3$ partial waves [19]. Thus it seems to be interesting to compare predictions for Nd scattering given by both potentials.

Besides the OPE-Gaussian and the AV18 models, we show in Sec. IV predictions based on two chiral forces at N^{4}LO, derived by Machleidt and collaborators [17] and by Epelbaum and collaborators [28,39]. In the case of the first of these forces the nonlocal regularization, applied directly in momentum space, was used. The regulator function is taken as $f(p', p) = \exp[-(\frac{p'}{\Lambda})^{2n} - (\frac{p}{\Lambda})^{2n}]$, where n depends on the regarded operators (e.g., $n = 4$ for the one-pion exchange potential). Three values of the cutoff parameter Λ (450, 500, and 550 MeV) were suggested for this potential and are also used in this paper. In the case of the N^{4}LO potential and $\Lambda = 500$ MeV, χ^2/data $= 1.15$ for the combined neutron-proton and proton-proton data in the energy range 0–290 MeV [17]. In this paper we show for the first time the predictions of this new chiral potential at N^{4}LO for the Nd elastic scattering observables. As mentioned above, in the approach of Refs. [28,39] the semilocal regularization of nuclear forces is performed in coordinate space with the regulator function $f(r) = \{1 - \exp[-(\frac{r}{R})^2]\}^6$, where r is the distance between nucleons and R is the regulator parameter. The authors of Ref. [28] suggested five values of the regulator, $R = 0.8$, 0.9, 1.0, 1.1, and 1.2 fm. The best description of the NN observables is achieved with $R = 0.9$ fm and $R = 1.0$ fm, and leads to χ^2/data ≈ 1.14 at $R = 0.9$ fm for the N^{4}LO force [25] when using the "3σ self-consistent database" from Ref. [18]. This value is comparable with the ones obtained for the semiphenomenological potentials.

III. THE OPE-GAUSSIAN PREDICTIONS FOR Nd SCATTERING AND THEIR STATISTICAL ERRORS

A. Determination of statistical uncertainty in a $3N$ system

To determine the theoretical uncertainty arising from the $2N$ potential parameters we took the following steps:

(1) We prepared various sets of the potential parameters. Actually, this step had been already taken by the Granada group as a part of their study of the statistical uncertainty of the ^{3}H binding energy. They provided us with 50 sets (S_i with $i = 1, \ldots, 50$) of 42 potential parameters (drawn from the multivariate normal distribution with known expectation values and covariance matrix) and one set of expectation values of potential parameters (S_0). Such a relatively big sample of 51 sets allows us to obtain statistically meaningful conclusions.

(2) For each set S_i ($i = 0, 1, \ldots, 50$) we calculated the deuteron wave function and the t matrix, solved, at each considered energy, the Faddeev equation (2.1), calculated the scattering amplitude [Eq. (2.2)], and finally computed observables. As a result the angular dependence of various scattering observables is known for each set of parameters S_i.

The predictions obtained in such a way allow us to study

(a) for a given energy E, an observable O, and a scattering angle θ, the empirical probability density function of the observable $O(E,\theta)$ resulting when various sets $S_i, (i = 1, \ldots, 50)$ are used;

(b) for a given observable O, both the angular and energy dependencies of results based on various sets S_i.

Based on these studies, we can conclude on the measure of statistical uncertainties and quality of the elastic Nd scattering data description. This is a content of the next two subsections.

B. Measure of statistical uncertainty

Our first task is to choose an estimator of the theoretical uncertainties in question. Due to the high complexity of calculations required to obtain the $3N$ scattering observables, we are not able *a priori* to determine analytically the probability distribution function of the resulting $3N$ predictions and consequently to choose the best estimator to describe the

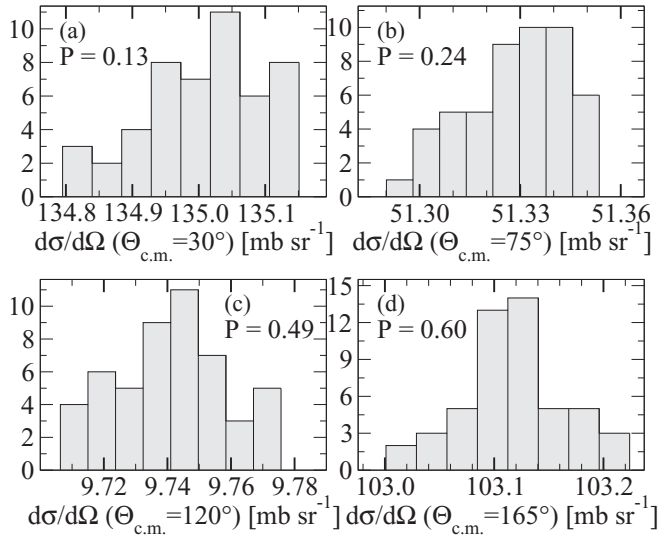

FIG. 1. The histograms and the P values for the Shapiro-Wilk test for the elastic Nd scattering differential cross section $d\sigma/d\Omega$ (mb sr^{-1}) at the incoming-nucleon laboratory energy $E = 13$ MeV and the scattering angles (a) $\theta_{\rm c.m.} = 30^\circ$, (b) $\theta_{\rm c.m.} = 75^\circ$, (c) $\theta_{\rm c.m.} = 120^\circ$, and (d) $\theta_{\rm c.m.} = 165^\circ$, obtained with 50 sets of the OPE-Gaussian potential parameters.

dispersion of results. In Figs. 1 and 2 we show the empirical distributions (histograms) of the cross section $d\sigma/d\Omega$ and the nucleon analyzing power A_y at the nucleon laboratory energy $E = 13$ MeV and at four center-of-mass (c.m.) scattering angles: $\theta_{\rm c.m.} = 30^\circ, 75^\circ, 120^\circ$, and 165°. The same observables at the same $\theta_{\rm c.m.}$ angles but at $E = 200$ MeV are shown in Figs. 3 and 4, respectively. It is clear that the distribution of the predictions cannot be regarded as the normal distribution.

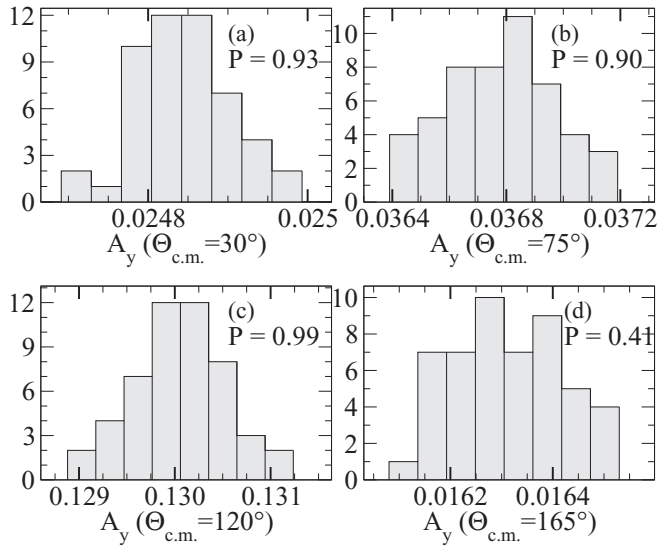

FIG. 2. The histograms and the P values for the Shapiro-Wilk test for the nucleon analyzing power A_y in Nd elastic scattering at the incoming-nucleon laboratory energy $E = 13$ MeV and the scattering angles (a) $\theta_{\rm c.m.} = 30^\circ$, (b) $\theta_{\rm c.m.} = 75^\circ$, (c) $\theta_{\rm c.m.} = 120^\circ$, and (d) $\theta_{\rm c.m.} = 165^\circ$, obtained with 50 sets of the OPE-Gaussian potential parameters.

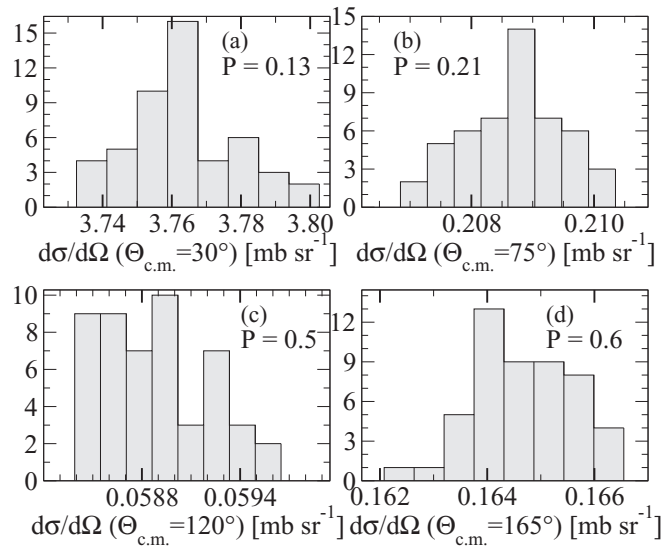

FIG. 3. The same as in Fig. 1 but at $E = 200$ MeV.

To obtain quantitative information on the distribution we have performed the Shapiro-Wilk test [47], which belongs to the strongest statistical tests of normality. As is seen from the obtained P values (the smaller the P value, the more unlikely the predictions are normally distributed) given in Figs. 1–4, in many cases the resulting distributions of the cross section and the nucleon analyzing power cannot be regarded with high confidence as normal distributions. This restricts a choice of the dispersion estimators: neither the commonly used confidence interval nor the usual estimators for the standard deviation can be used directly as they are tailored to the normal distribution. Thus we considered the following estimators for the statistical error of the observable $O(E,\theta)$ (at a given energy and a scattering angle):

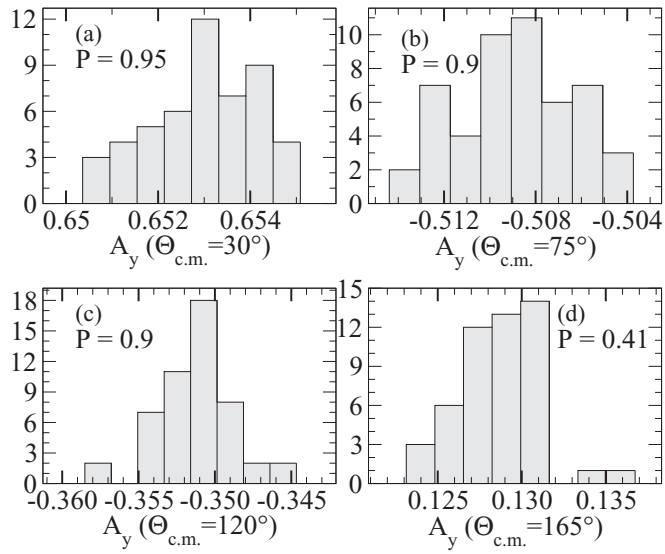

FIG. 4. The same as in Fig. 2 but at $E = 200$ MeV.

TABLE I. The differential cross section $d\sigma/d\Omega$ obtained with the expectation values of the OPE-Gaussian potential parameters (set S_0), various estimators of its dispersion (see text), and mean values taken from 50 ($M_{100\%}$) or 34 ($M_{68\%}$) predictions. In case of the sample standard deviation $\sigma(d\sigma/d\Omega)$ also the relative magnitude $\sigma(d\sigma/d\Omega)/[d\sigma/d\Omega(S_0)] \times 100\%$ is shown in parentheses. All predictions are given in mb sr^{-1}.

E (MeV)	$\theta_{\rm c.m.}$ (deg)	$d\sigma/d\Omega(S_0)$	$\frac{1}{2}\Delta_{100\%}$	$\frac{1}{2}\Delta_{68\%}$	$\frac{1}{2}$IQR	$\sigma(d\sigma/d\Omega)$	$M_{100\%}$	$M_{68\%}$
13.0	30	134.9970	0.1780	0.1025	0.0635	0.0954 (0.132%)	135.0040	135.0100
	75	51.3274	0.0315	0.0153	0.0110	0.0149 (0.061%)	51.3283	51.3295
	120	9.7437	0.0347	0.0181	0.0118	0.0179 (0.356%)	9.7421	9.7420
	165	103.1210	0.1085	0.0420	0.0230	0.0462 (0.105%)	103.1190	103.1190
65.0	30	23.7000	0.1785	0.0812	0.0569	0.0824 (0.753%)	23.7137	23.7092
	75	2.3630	0.0134	0.0060	0.0040	0.0057 (0.568%)	2.3630	2.3630
	120	0.7787	0.0035	0.0015	0.0011	0.0016 (0.451%)	0.7786	0.7785
	165	4.7537	0.0174	0.0076	0.0060	0.0075 (0.366%)	4.7532	4.7535
200.0	30	3.7626	0.0351	0.0164	0.0097	0.0162 (0.325%)	3.7634	3.7625
	75	0.2088	0.0018	0.0008	0.0005	0.0008 (0.839%)	0.2087	0.2087
	120	0.0585	0.0006	0.0004	0.0003	0.0003 (1.069%)	0.0589	0.0589
	165	0.1645	0.0022	0.0009	0.0007	0.0009 (1.356%)	0.1647	0.1647

(1) $\frac{1}{2}\Delta_{100\%} \equiv \frac{1}{2}[\max_i(O_i) - \min_i(O_i)]$, where the minimum and maximum are taken over all predictions based on different sets of the NN potential parameters S_i, $i = 1,2,\ldots,50$.

(2) $\frac{1}{2}\Delta_{68\%} \equiv \frac{1}{2}[\max_i(O_i) - \min_i(O_i)]$, where the minimum and maximum are taken over 34 (68% of 50) predictions based on different sets of the NN potential parameters. The set of 34 observables is constructed by disposing of the 8 smallest and the 8 biggest predictions for the observable $O(E,\theta)$.

(3) $\frac{1}{2}$IQR: half of the standard estimator of the interquartile range being the difference between the third and the first quartile IQR $= Q_3 - Q_1$. For the sample of size 50 this corresponds to taking half of the difference between the predictions on 37th and 13th positions in a sample sorted in ascending order. The flexibility in applying this measure to the nonnormal distribution is a great asset of the IQR.

(4) $\sigma(O)$: the sample standard deviation $\sigma(O) = \sqrt{\frac{1}{n-1}\sum_{i=1}^{n}(x_i - \bar{x})^2}$, where $\bar{x}$ is the usual mean value. The disadvantage of this estimator is that on formal grounds it cannot be applied to samples from an arbitrary probability distribution.

The estimators $\frac{1}{2}\Delta_{100\%}$ and $\sigma(O)$ are sensitive to possible outliers in the sample, and thus taking them as estimators of dispersion can lead to overestimation of the statistical error. On the other hand the IQR is calculated using only half of the elements in the sample and thus can lead to underestimation of the theoretical uncertainty. Thus we decided to adapt $\frac{1}{2}\Delta_{68\%}$ as an optimal measure of predictions' dispersion and consequently as an estimator of the theoretical uncertainty in question. The same choice was made in a study of the statistical error of the ^3H binding energy in Ref. [46]. The similarity to the standard deviation is one more advantage of $\frac{1}{2}\Delta_{68\%}$ since the comparison of the theoretical errors with the experimental (statistical) uncertainties, delivered usually in the form of standard deviations, is finally unavoidable.

However, in Table I we compare values of the above mentioned estimators for the Nd elastic scattering differential cross section at three energies of the incoming nucleon and at four c.m. scattering angles. By definition $\frac{1}{2}\text{IQR} \leqslant \frac{1}{2}\Delta_{68\%} \leqslant \frac{1}{2}\Delta_{100\%}$ and indeed this is observed in Table I. The magnitudes of $\frac{1}{2}\Delta_{68\%}$ are very close to the measure based on the sample standard deviation $\sigma(d\sigma/d\Omega)$ and in practice it does not matter which of these estimators is used. The relative uncertainty (exemplified in Table I for the sample standard deviation) remains below 1% for all scattering angles at $E = 13$ MeV and $E = 65$ MeV, and only slightly exceeds it at $E = 200$ MeV. In Table I we also show values of the differential cross section obtained with the central values of the OPE-Gaussian potential parameters and mean values of predictions calculated separately for the 50 ($M_{100\%}$) or 34 ($M_{68\%}$) sets of parameters S_i. Also here in most of the cases $d\sigma/d\Omega(S_0) \approx M_{100\%} \approx M_{68\%}$, which shows that the predictions based on sets S_i for $i \neq 0$ cluster around $d\sigma/d\Omega(S_0)$ evenly. The other observables behave in a similar way.

C. Nucleon-deuteron elastic scattering observables from the OPE-Gaussian model

In the following we present predictions obtained with the OPE-Gaussian NN interaction for various observables in the elastic neutron-deuteron scattering process at incoming-nucleon laboratory energies $E = 13$, 65, and 200 MeV. We will focus on the elastic scattering cross section $d\sigma/d\Omega$, the nucleon vector analyzing power A_y, the nucleon-to-nucleon spin transfer coefficients $K_y^{y'}$, and the spin correlation coefficients $C_{y,y}$. However, we will also give examples for other observables.

The Nd cross section is shown in Fig. 5. Apart from the solid line which represents predictions based on the OPE-Gaussian force when the expectation values of its parameters (set S_0) are used, we also show a red band representing the range of predictions obtained with the same 34 sets S_i as used to calculate $\frac{1}{2}\Delta_{68\%}$, and a blue dashed curve showing results obtained with the AV18 interaction. The nucleon-deuteron data

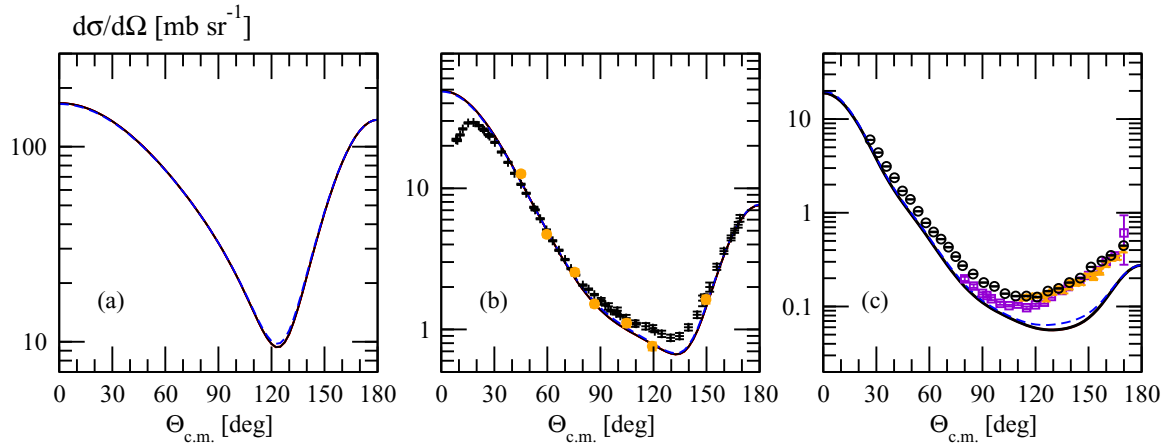

FIG. 5. The Nd elastic scattering cross section $d\sigma/d\Omega$ (mb sr^{-1}) at the incoming-nucleon laboratory energies (a) $E = 13$ MeV, (b) $E = 65$ MeV, and (c) $E = 200$ MeV as a function of the c.m. scattering angle $\theta_{\text{c.m.}}$. The black curve represents predictions obtained with the central values of the OPE-Gaussian parameters, the red band reflects statistical uncertainty discussed in this subsection, and the blue dashed curve represents predictions based on the AV18 force. The data are in (b) from Ref. [50] (pd black pluses) and [51] (nd orange circles) and in (c) from Ref. [52] (pd, $E = 198$ MeV, violet squares), Ref. [53] (pd, $E = 180$ MeV, orange $\times$'s), and Ref. [54] (pd, $E = 198$ MeV, black circles).

(at the same or nearby energies) are also added for the sake of comparison. The predictions based on the OPE-Gaussian force are in agreement with the predictions based on the AV18 potential. Only small ($\approx$3.9% at $E = 13$ MeV and $\approx$3.5% at $E = 200$ MeV) differences are seen in the minimum of the cross section. Similarly to the AV18, the OPE-Gaussian model clearly underestimates the data at two higher energies, reflecting the known fact of growing importance of a $3N$ force [48,49]. The statistical error arising from the uncertainty of the NN force parameters is in all cases very small, and red bands are hardly visible in Fig. 5.

The OPE-Gaussian force delivers predictions which are very close to the AV18 results also for the most of the polarization observables at the energies studied here. Likewise the dispersion of predictions remains small for most of the polarization observables. Below we discuss a few of them, choosing mainly ones with the largest statistical uncertainties.

Let us start, however, with the nucleon analyzing power A_y, shown in Fig. 6. Here the uncertainties remain negligible at all energies and also the differences between predictions based on the OPE-Gaussian force and the ones obtained with the AV18 potential are tiny. Thus we see that the OPE-Gaussian model does not deliver any hint on the nature of the A_y puzzle at $E = 13$ MeV.

We have chosen the nucleon-to-nucleon spin transfer coefficient $K_y^{y'}$ and the spin correlation coefficient $C_{y,y}$ to demonstrate, in Figs. 7 and 8, respectively, changes of the statistical errors when increasing the reaction energy. For both observables dispersion of the results grows with energy, and while at lowest energy $E = 13$ MeV it is negligible, at $E = 200$ MeV its size is bigger, although it remains small ($\frac{1}{2}\Delta_{68\%} < 0.5\%$). In the case of $C_{y,y}$ comparison with the data reveals that the spread of the OPE-Gaussian results is still smaller than uncertainties of experimental results.

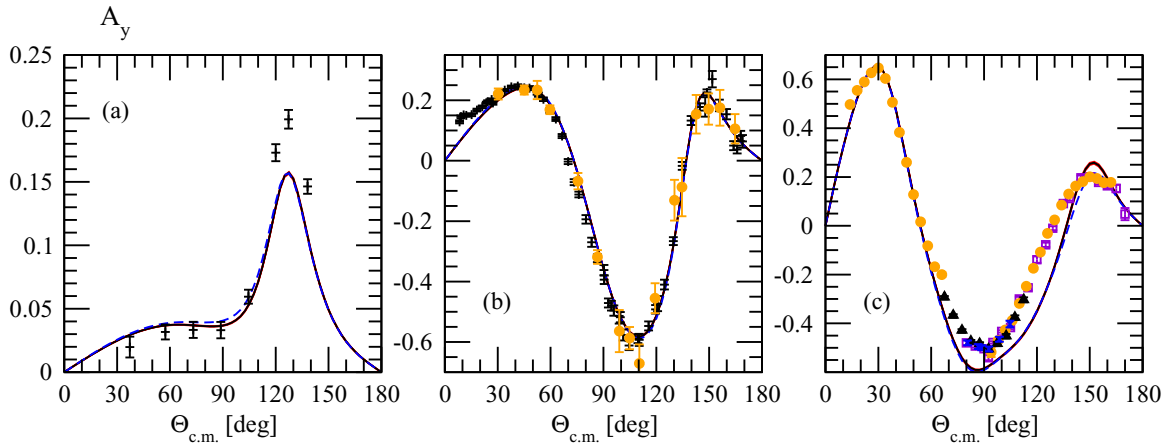

FIG. 6. The nucleon analyzing power A_y for Nd elastic scattering at the same energies as used in Fig. 5 as a function of the c.m. scattering angle $\theta_{\text{c.m.}}$. Curves and band as in Fig. 5. The data are in (a) are from Ref. [55] (nd black pluses), in (b) from Ref. [50] (pd black pluses) and Ref. [51] (nd orange circles), and in (c) from Ref. [52] (pd violet squares), Ref. [3] (pd $E = 200$ MeV orange circles), Ref. [56] (pd $E = 197$ MeV black up-triangles), and Ref. [57] (pd blue $\times$'s).

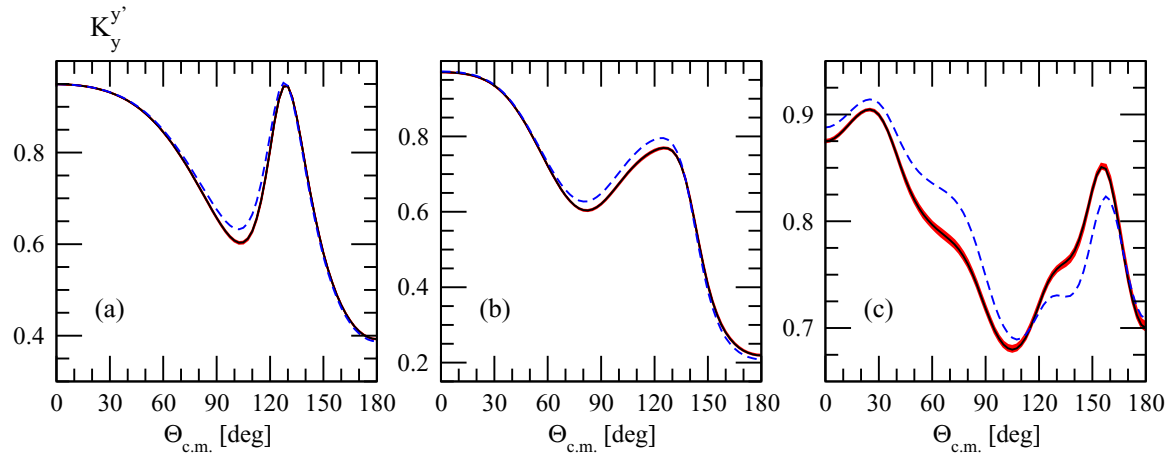

FIG. 7. The nucleon to nucleon spin transfer coefficient $K_y^{y'}$ at the incoming-nucleon laboratory energies (a) $E = 13$ MeV, (b) $E = 65$ MeV, and (c) $E = 200$ MeV as a function of the c.m. scattering angle $\theta_{\text{c.m.}}$. See Fig. 5 for a description of band and curves.

In Fig. 9 we show two observables for which the difference between the AV18 predictions and the OPE-Gaussian results is especially big already at the two lower energies. They are the spin correlation coefficient $C_{xx,y}$-$C_{yy,y}$ at $E = 13$ MeV and the deuteron-to-nucleon spin transfer coefficient $K_{yz}^{x'}$ at $E = 65$ MeV. The difference between the two predictions amounts to ≈19% at the minimum of $C_{xx,y}$-$C_{yy,y}$, while the statistical error of the OPE-Gaussian results is only ≈2%. For $K_{yz}^{x'}$ these differences amount to ≈23% and ≈3%, respectively. We see that even in these two cases the statistical uncertainty remains much smaller than the uncertainty related to using various models of the NN interaction.

The statistical errors grow with the reaction energy. Thus in Fig. 10 we show for $E = 200$ MeV a few observables with the largest uncertainties. Besides the spin transfer coefficient $K_y^{y'}$ already shown in Fig. 7, they are the deuteron tensor analyzing powers T_{21} and T_{22} and the nucleon to deuteron spin transfer coefficient $K_y^{x'x'}$-$K_y^{y'y'}$. While the bands representing the theoretical uncertainties are clearly visible, they still remain small compared to the experimental errors for both analyzing powers. The differences between predictions based on the AV18 potential and the OPE-Gaussian force are small. This is true also for the other Nd elastic scattering observables both at $E = 200$ MeV and at the lower energies, so we conclude that the OPE-Gaussian force yields a description of this process similar to the AV18 potential.

IV. COMPARISON OF VARIOUS THEORETICAL UNCERTAINTIES IN Nd SCATTERING

It is interesting to compare the statistical error $\frac{1}{2}\Delta_{68\%}$ obtained in the previous section with the other uncertainties (like the uncertainty arising from using the various models of nuclear interaction, the uncertainty introduced by the partial wave decomposition approach, the truncation errors of chiral predictions, and the uncertainties originating in the cutoff dependence of chiral forces) present in the elastic Nd scattering studies and specifically in our approach.

The accuracy of predictions arising from the algorithms used in our numerical scheme, which comprises, among others,

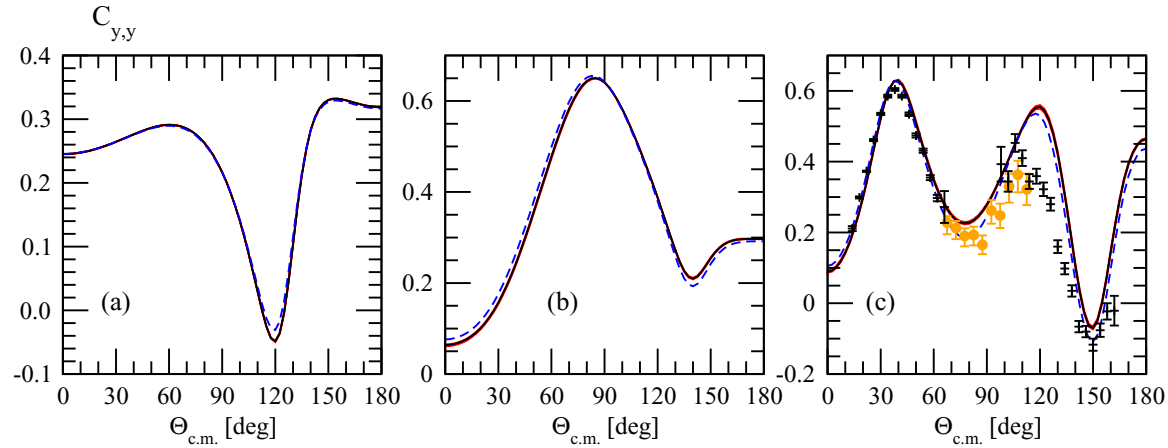

FIG. 8. The spin correlation coefficient $C_{y,y}$ at the incoming-nucleon laboratory energies (a) $E = 13$ MeV, (b) $E = 65$ MeV, and (c) $E = 200$ MeV as a function of the c.m. scattering angle $\theta_{\text{c.m.}}$. See Fig. 5 for a description of band and curves. In (c) data are from Ref. [56] (pd $E = 197$ MeV, orange circles) and Ref. [3] (pd $E = 200$ MeV, black pluses).

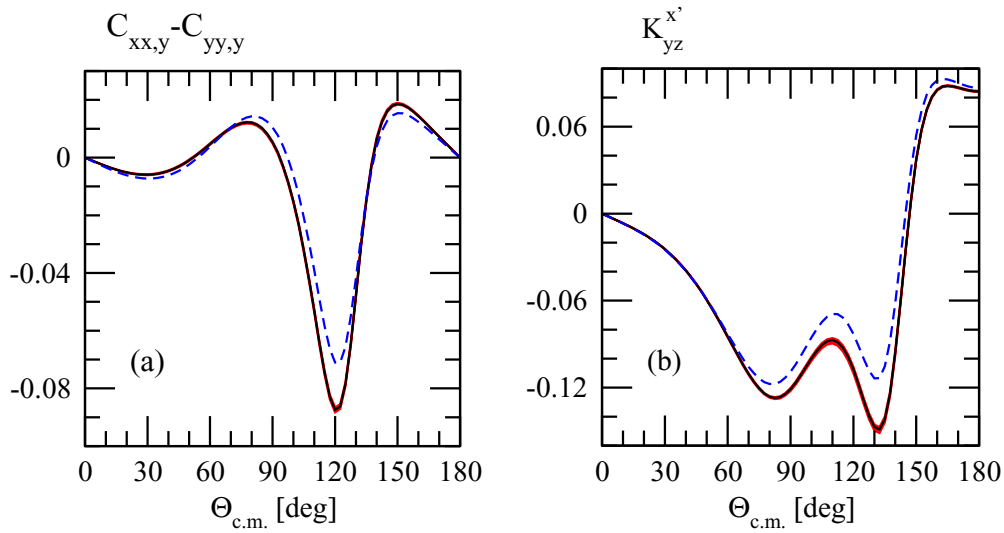

FIG. 9. The spin correlation coefficient $C_{xx,y}$-$C_{yy,y}$ at the incoming-nucleon laboratory energy $E = 13$ MeV (a) and the deuteron to nucleon spin transfer coefficient $K_{yz}^{x'}$ at the incoming-nucleon laboratory energy $E = 65$ MeV (b) as a function of the c.m. scattering angle $\theta_{\text{c.m.}}$. Curves and band are as in Fig. 5.

numerical integrations, interpolations, and series summations, is well under control. This has been tested, e.g., by using various grids of mesh points, or more generally by benchmark calculations involving different methods to treat Nd scattering [9–12]. The main contribution to theoretical uncertainties comes in our numerical realization from using a truncated set of partial waves. Typically we restrict ourselves to partial waves with the two-body total orbital momentum $j \leqslant 5$. Predictions for observables converge with increasing j, as was documented, e.g., in [44]. In the following we compare the OPE-Gaussian predictions, shown in the previous section, based on all two-body channels up to $j = 5$ with the predictions based on all channels up to $j = 4$ only to remind the reader of some facts about the convergence of our approach. However, since the differences between (not shown here) predictions based on all channels up to $j = 6$ and those with $j_{\max} = 5$ are, based on results with other NN potentials, smaller than this for $j_{\max} = 5$ and $j_{\max} = 4$ predictions, the latter difference very likely overestimates the uncertainty arising from our computational scheme. A recent work [58] compares predictions for the elastic Nd scattering, based however only on the driving term of Eq. (2.1), obtained within the partial wave formalism with the ones from the "three-dimensional" approach, i.e., the approach which totally avoids the partial wave decomposition and uses momentum vectors. A very good agreement between the partial waves based results and the "three-dimensional" ones confirms that neglecting the higher partial waves in the calculations presented here practically does not affect our predictions.

Next, we would like to focus on the truncation errors and the cutoff dependence present in the chiral calculations and last but not least on the differences between predictions based on various models of the nuclear two-body interaction.

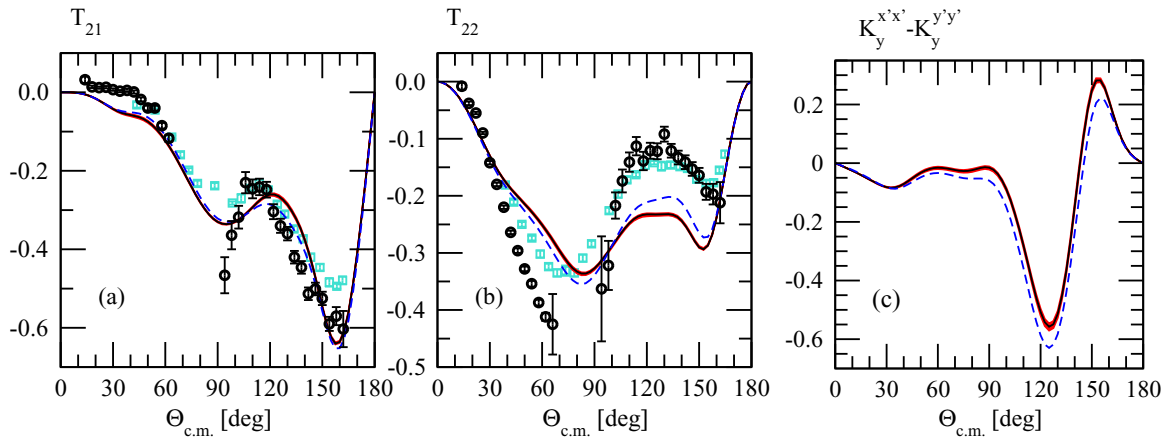

FIG. 10. The deuteron tensor analyzing powers T_{21} (a) and T_{22} (b) and the nucleon-to- deuteron spin transfer coefficient $K_y^{x'x'}$-$K_y^{y'y'}$ (c) for $E = 200$ MeV as a function of the center-of-mass scattering angle $\theta_{\text{c.m.}}$. See Fig. 5 for a description of bands and curves. The T_{21} and T_{22} data are from Ref. [1] (pd $E = 186.6$ MeV turquoise squares) and Ref. [3] (pd $E = 200$ MeV black circles).

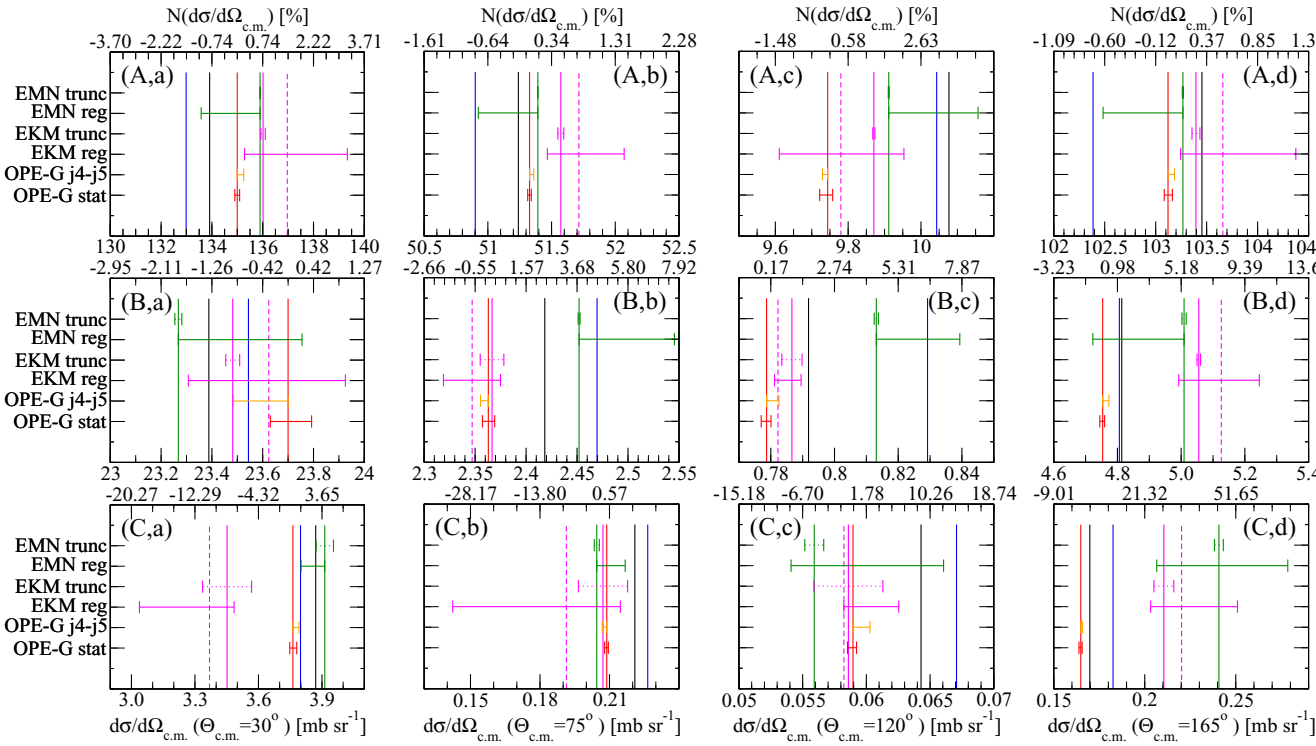

FIG. 11. The Nd elastic scattering differential cross section and various theoretical uncertainties at four scattering angles: $\theta_{\mathrm{c.m.}} = 30^\circ$ [first column (a)], 75° [second column (b)], 120° [third column (c)], and 165° [fourth column (d)] and at three scattering energies: $E = 13$ MeV [the upper row (A)], $E = 65$ MeV [the middle row (B)], and $E = 200$ MeV [the bottom row (C)]. The x axis at the bottom shows the values of the cross section and the x axis at the top shows the relative difference of predictions with respect to the OPE-Gaussian results. The vertical lines show the position of the cross section obtained with the AV18 force (black line), the OPE-Gaussian force (red line), the E-M-N N^{4}LO $\Lambda = 500$ MeV force (green line), the CD-Bonn potential (blue line), the E-K-M N^{4}LO $R = 0.9$ fm force (magenta solid line), and the E-K-M N^{4}LO $R = 1.0$ fm force (magenta dashed line). The horizontal lines represent (from the bottom) the statistical error (red line), the difference between the OPE-Gaussian predictions with $j_{\max} = 5$ and $j_{\max} = 4$ (orange line), the regulator dependence for the E-K-M force (magenta solid line), the truncation error for the E-K-M force (magenta dashed line), the regulator dependence for the E-M-N force (green solid line), and, at the top, the truncation error for the E-M-N potential (green dashed line); see text for details.

To estimate two types of theoretical uncertainties present when chiral potentials are used, we calculated the elastic Nd scattering observables using two NN interactions at the N^{4}LO: one delivered by Epelbaum *et al.* [39] (E-K-M force) and the other derived by Entem *et al.* [17] (E-M-N force). In the case of the E-K-M model a semilocal regularization with a cutoff parameter R in the range between 0.8 and 1.2 fm is used and the breakdown scale of the χEFT is 0.4–0.6 GeV [39]. The E-M-N model uses a chiral breaking scale of 1 GeV, and the cutoff parameter Λ for nonlocal regularization lies between 450 and 550 MeV [17].

The truncation errors $\delta(O)^{(i)}$ of an observable O at ith order of the chiral expansion, with $i = 0,2,3,\ldots$, when only two-body interaction is used, can be estimated as [29]

$$\begin{aligned}
\delta(O)^{(0)} &\geqslant \max(Q^2|O^{(0)}|, |O^{(i\geqslant 0)} - O^{(j\geqslant 0)}|),\\
\delta(O)^{(2)} &= \max(Q^3|O^{(0)}|, Q|\Delta O^{(2)}|, |O^{(i\geqslant 2)} - O^{(j\geqslant 2)}|),\\
\delta(O)^{(i)} &= \max(Q^{i+1}|O^{(0)}|, Q^{i-1}|\Delta O^{(2)}|, Q^{i-2}|\Delta O^{(3)}|),\\
&\quad \text{for } i \geqslant 3, \qquad (4.1)
\end{aligned}$$

where Q denotes the chiral expansion parameter, $\Delta O^{(2)} \equiv O^{(2)} - O^{(0)}$, and $\Delta O^{(i)} \equiv O^{(i)} - O^{(i-1)}$ for $i \geqslant 3$. In addition conditions $\delta(O)^{(2)} \geqslant Q\delta(O)^{(0)}$ and $\delta(O)^{(i)} \geqslant Q\delta(O)^{(i-1)}$ for $i \geqslant 3$ are imposed on the truncation errors $\delta(O)^{(i)}$ in the case when, at higher orders, $3N$ force is not included in calculations [29].

The uncertainty arising from the cutoff dependence can be easily quantified: we just take the difference between the minimal and the maximal predictions, separately for the E-K-M force and for the E-M-N model. However, one has to be aware that in the case of the E-K-M force cutoff values between $R = 0.9$ fm and $R = 1.0$ fm are preferred in the $2N$ system. Thus in the following we separately discuss the whole range of regulator values ($0.8 \leqslant R \leqslant 1.2$ fm) and the range restricted to $0.9 \leqslant R \leqslant 1.0$ fm only.

To estimate the uncertainty arising from using various models of nuclear forces, we do not introduce any separate measure but just show the differences between predictions obtained with various interactions. Admittedly, the authors of Ref. [20] suggest in such a case to calculate the estimator of standard deviations, but this is valid only under assumptions of the same quality of all interaction models, which is not clear in the case of the calculations presented here.

A systematical review of various uncertainties for the differential cross section $d\sigma/d\Omega$, the nucleon analyzing power

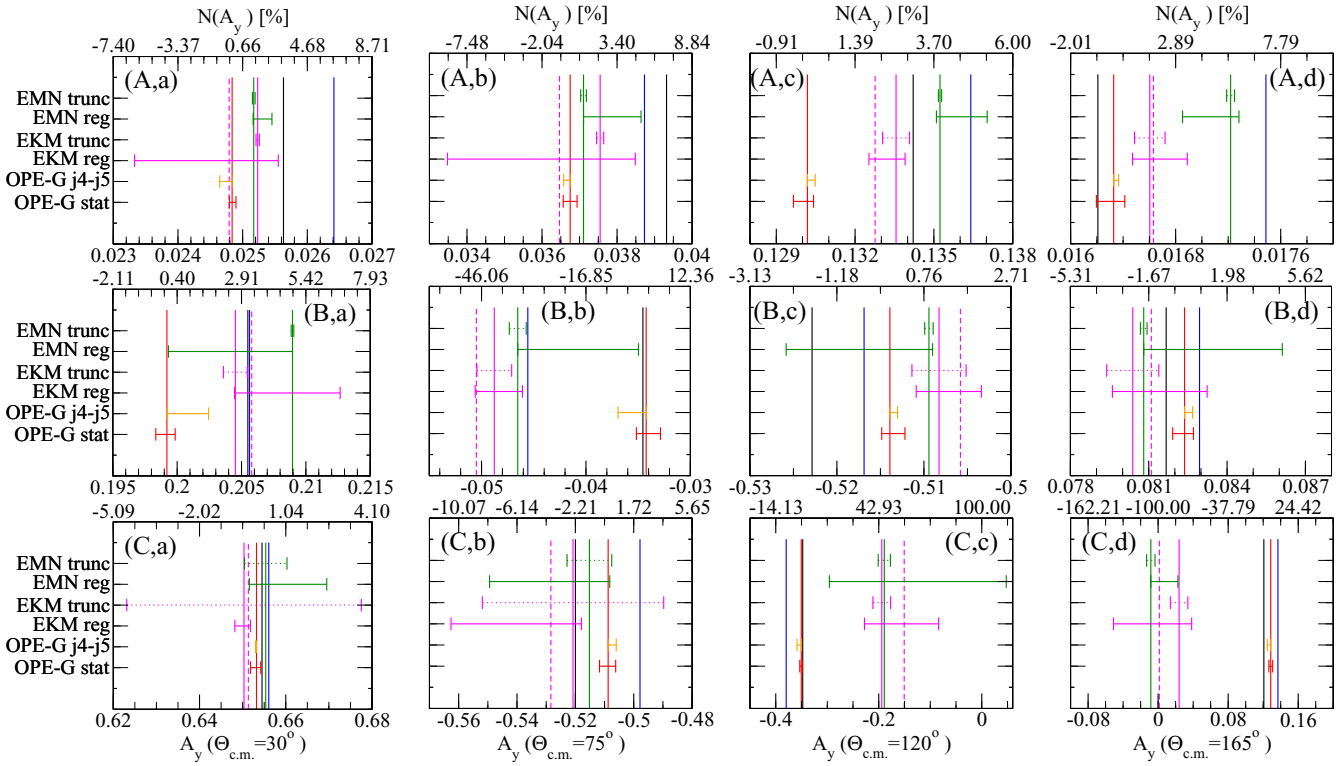

FIG. 12. The same as in Fig. 11 but for the nucleon analyzing power A_y.

A_y, the deuteron tensor analyzing power T_{22}, and the spin correlation coefficient $C_{y,y}$ is given in Figs. 11–14, respectively. In these figures, in each subplot, the predicted value of the observable is given at the bottom horizontal axis and the vertical lines are used to mark predictions based on different NN forces; the length of these lines has no meaning. The top horizontal axis shows the percentage relative difference $N(O)$ with respect to the OPE-Gaussian prediction and its ticks are calculated as $\tilde{x} = (\frac{x - O_{\text{OPE-Gaussian}}}{O_{\text{OPE-Gaussian}}}) \times 100 \times \text{sgn}(O_{\text{OPE-Gaussian}})$, where x are the tick values shown at the bottom axis. In addition, for the sake of figures' clarity, the $\tilde{x}$'s are rounded to the two digits only. Note that the magnitude of such a relative difference depends on the magnitude of the OPE-Gaussian prediction and can increase to infinity as the OPE-Gaussian prediction approaches zero. The OPE-Gaussian results (at the central values of the parameters) are represented by vertical red lines, the AV18 ones by the black line, the CD-Bonn predictions by the blue line, the E-K-M N^{4}LO $R = 0.9$ fm results by the magenta solid line, the E-K-M N^{4}LO $R = 1.0$ fm ones by the magenta dashed line, and the E-M-N N^{4}LO $\Lambda = 500$ MeV ones by the green line. Horizontal lines represent magnitudes of various theoretical uncertainties and, starting from the bottom, they are statistical error for the OPE-Gaussian model (the red line), difference between OPE-Gaussian predictions based on the $j_{\max} = 5$ and $j_{\max} = 4$ calculations (the orange line), regulator dependence for the E-K-M N^{4}LO force in range $R = 0.8$–1.2 fm (the solid magenta line), the truncation error for the E-K-M N^{4}LO $R = 0.9$ fm model (the dashed magenta line), regulator dependence for the E-M-N N^{4}LO force in the range $\Lambda = 450$–550 MeV (the solid green line), and truncation error for the E-M-N N^{4}LO $\Lambda = 500$ MeV potential (the dashed green line). Further, subplots in various rows in Figs. 11–14 show predictions at different incoming-nucleon laboratory energies, which are $E = 13$ MeV (top), $E = 65$ MeV (middle), and $E = 200$ MeV (bottom). Finally, the various columns show predictions at different scattering angles: 30°, 75°, 120°, and 165° moving from the left to the right.

An analysis of Figs. 11–14 leads to the following conclusions:

(1) In general, all models investigated here provide similar results, which differ only by a few percent at lower energies, but differences between predictions grow with the increasing energy. There is no single model which gives systematically the smallest or the biggest value. There are also no two models whose predictions for all the cases lie close to each other. Note, the above statements describe general trends but exceptions from this pattern for specific observables and angles are possible.

(2) At all energies the dominant theoretical uncertainty is the one arising from using various models of the nuclear interaction.

(3) The statistical errors for the OPE-Gaussian predictions are small (and with no practical importance) for all the considered observables and energies.

(4) The difference between $j_{\max} = 5$ and $j_{\max} = 4$ predictions, as expected, grows with energy; however, it remains small when compared to other uncertainties, even at $E = 200$ MeV (with the only exceptions of the T_{22} at 200 MeV and $C_{y,y}$ at 65 MeV). Thus the

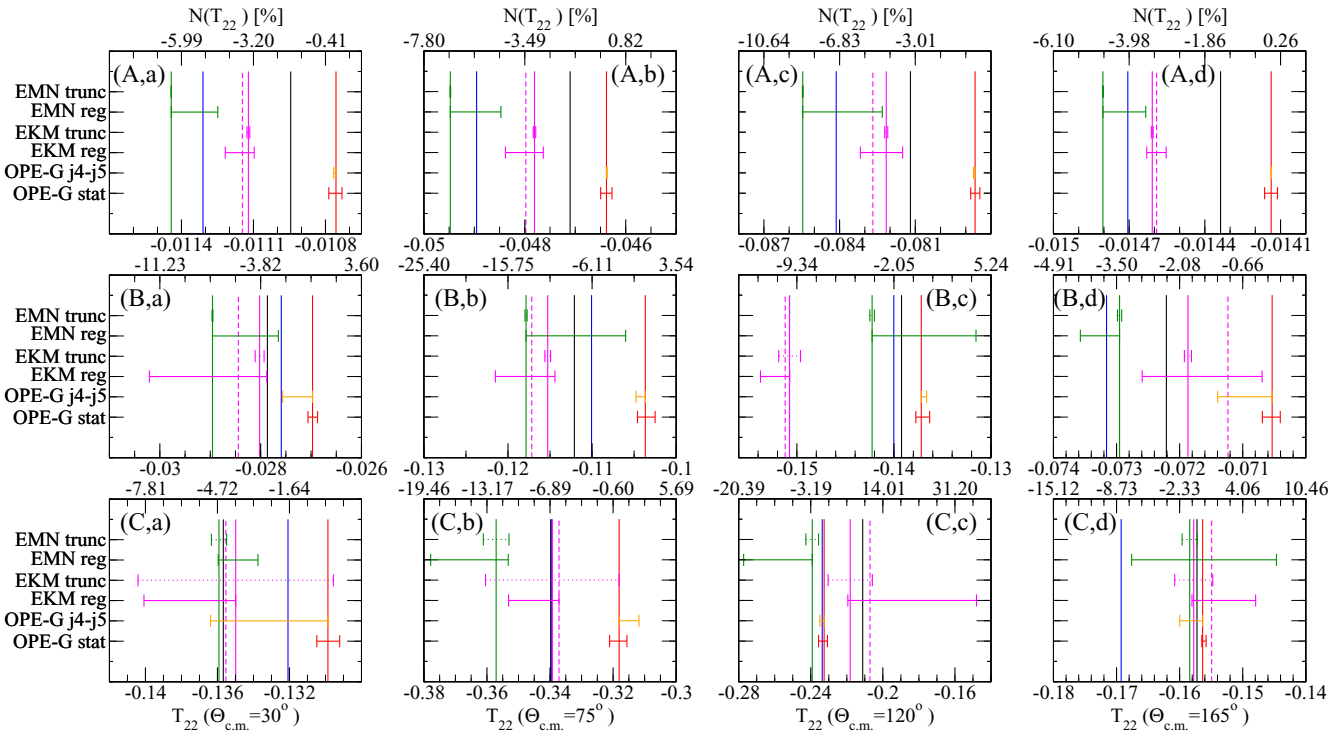

FIG. 13. The same as in Fig. 11 but for the deuteron tensor analyzing power T_{22}.

uncertainty bound with partial wave decomposition and numerical performance is also negligible.

(5) The OPE-Gaussian predictions based on the central values are always inside the range given by the statistical errors. The E-K-M results show monotonic behavior of the predicted observables with the regulator value. In the case of the E-M-N force the middle value of regulator ($\Lambda = 500$ MeV) delivers extreme (among the E-M-N ones) predictions in many cases.

(6) The difference between predictions based on the two chiral N^{4}LO models used (E-K-M and E-M-N) is not smaller than the difference between any other pair of predictions based on different NN potentials. This suggests that there are substantial differences in the construction of each of these models. Thus it seems mandatory to regard these models independently, as two different models of nuclear forces.

(7) In numerous cases the two chiral approaches deliver results separated from each other by more than the estimated uncertainty for their predictions. This again points to differences between the two chiral potentials (and/or to an underestimation of the corresponding total theoretical uncertainties).

(8) In the case of both chiral models, the dominant uncertainty at lower energies arises from the cutoff dependence. This uncertainty is much bigger than the remaining types of errors, except for differences between various models. At higher energies the truncation errors are also important in some specific cases, e.g., the differential cross section at $\theta_{\rm c.m.} = 120^\circ$ at $E = 200$ MeV. In the case of A_y at $E = 200$ MeV and smaller angles, the truncation errors exceed the regulator dependence for the E-K-M potential.

(9) In the case of the N^{4}LO E-K-M potential, the difference between predictions for $R = 0.9$ fm and $R = 1.0$ fm (i.e., at the two preferred values of the regulator in the NN system) is of the same size as the typical difference between any other pair of predictions, what shows strong sensitivity of the observables to the regulator parameter.

(10) Comparing the cutoff dependence of both chiral models we can conclude that the dispersion of their predictions behaves for the two models in a correlated way; i.e., a big cutoff dependence for the E-M-N force usually appears together with a big cutoff dependence for the E-K-M potential.

(11) The truncation errors for the E-M-N force are smaller than these for the E-K-M interaction. The reason for this is the bigger value of the chiral breaking scale in the E-M-N approach, which results in different values of Q parameter in Eq. (4.1).

Next, it is interesting to compare the size of the theoretical errors presented in Figs. 11–14 to experimental errors of available data. In order not to leave the reader with the impression that the modern theoretical models of nuclear interactions yield a chaotic description of the Nd scattering observables, in Fig. 15 we compare, in a few examples, previously presented predictions with the experimental results. This establishes an absolute scale in which one should examine the problem of discrepancies between various theoretical models.

Examples given in Fig. 15 show various possible locations of theoretical predictions and data. The differential cross

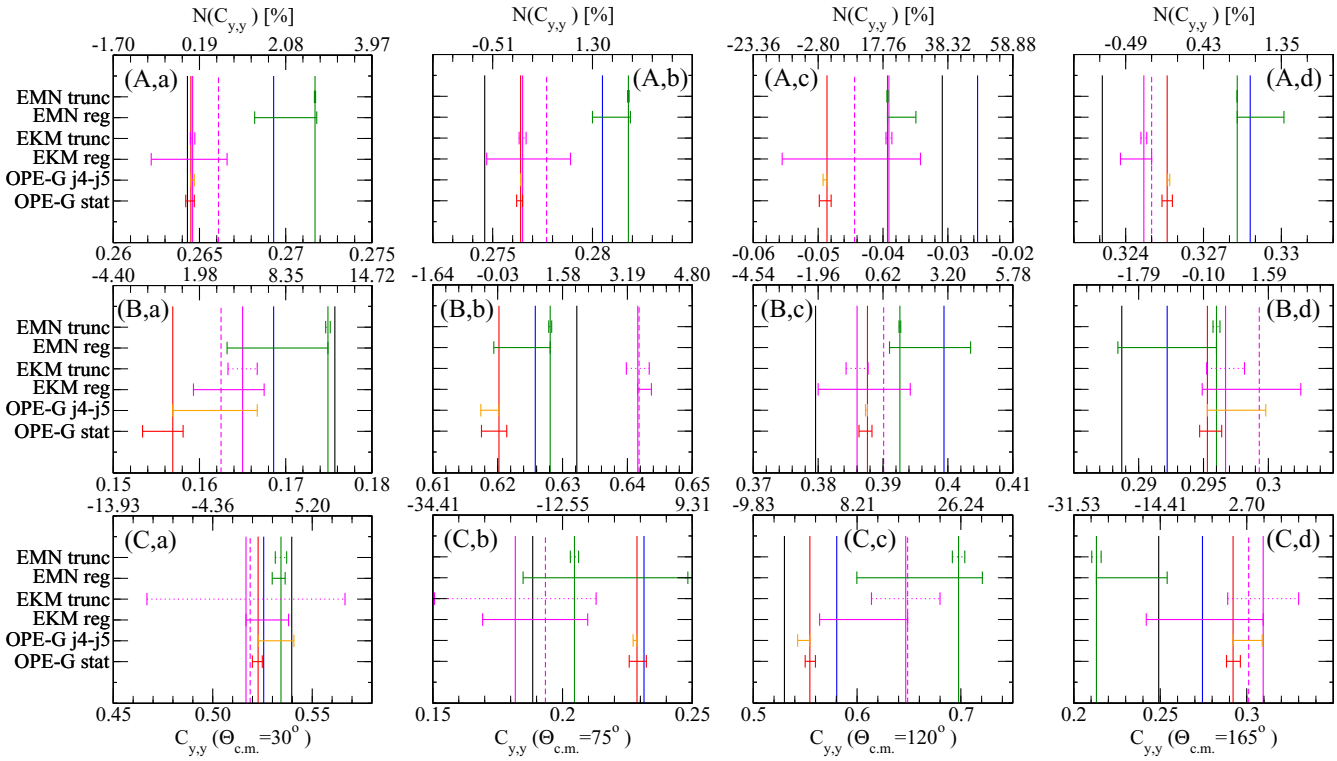

FIG. 14. The same as in Fig. 11 but for the spin correlation coefficient $C_{y,y}$.

section at $E = 65$ MeV and $E = 200$ MeV at the scattering angle $\theta_{\text{c.m.}} = 120^\circ$ is shown in the upper row and the analyzing power A_y for the same angle and energies is displayed below. In the case of the cross section we see that at $E = 65$ MeV there are discrepancies between various theoretical predictions and the data of different measurements. While the theoretical predictions are close one to each other, the data are scattered. One experimental point overlaps within its statistical error with some of the predictions, another one would be in agreement with predictions within 3σ distance, and the remaining experimental point is further from the data by more than its 3σ uncertainty. At $E = 200$ MeV a clear discrepancy between all predictions, which again are close together, and all data is observed. This discrepancy can be traced back to action of $3N$ force at higher energies [48,49]. The picture is more complex for the analyzing power. Here, at $E = 65$ MeV the experimental data and predictions differ by more than experimental error but they already agree within the 2σ range. At $E = 200$ the experimental statistical error is much smaller than the distances between various theoretical predictions, and the uncertainties related to the chiral forces. Such a mixed pattern clearly calls for further work to reduce both the theoretical and experimental uncertainties to avoid misleading conclusions about the properties of nuclear interactions. The examples presented here at one scattering angle only show that it is much more reliable to draw conclusions based on a comparison of predictions with data in a wider range of scattering angles and at different energies. Especially, these examples do not contradict strong effects of the $3N$ force in the minimum of the differential cross section at higher energies [48,49]. Such conclusions are based on a systematic comparison of predictions with the data at numerous scattering angles and energies.

V. SUMMARY

We have employed the OPE-Gaussian potential of the Granada group to describe the elastic Nd scattering at energies up to 200 MeV. The OPE-Gaussian potential is one of the first models of nuclear forces for which the covariance matrix of its free parameters is known. This gives an excellent opportunity to study the propagation of uncertainties from the $2N$ potential parameters to $3N$ observables. Therefore, for the same process, we also studied the statistical errors of our predictions.

The description of data delivered by the OPE-Gaussian force is in quantitative agreement with the picture obtained using other NN potentials, especially the AV18 model, which resembles by construction the OPE-Gaussian potential. We found only small discrepancies between predictions of these forces, especially at the highest energy investigated here, $E = 200$ MeV, which can very probably originate from a slightly different behavior of the phase shifts for the AV18 and the OPE-Gaussian potentials at energies above $\approx$150 MeV. It should be noted that the procedure of fixing free parameters for the OPE-Gaussian force has been performed with great care for statistical correctness and covers new $2N$ data not included when fixing the AV18 parameters.

In order to obtain the theoretical uncertainty of our predictions arising from the uncertainty of the NN potential parameters, we employed the statistical approach: we computed the Nd scattering observables using 50 sets of the OPE-Gaussian potential parameters obtained from a suitable

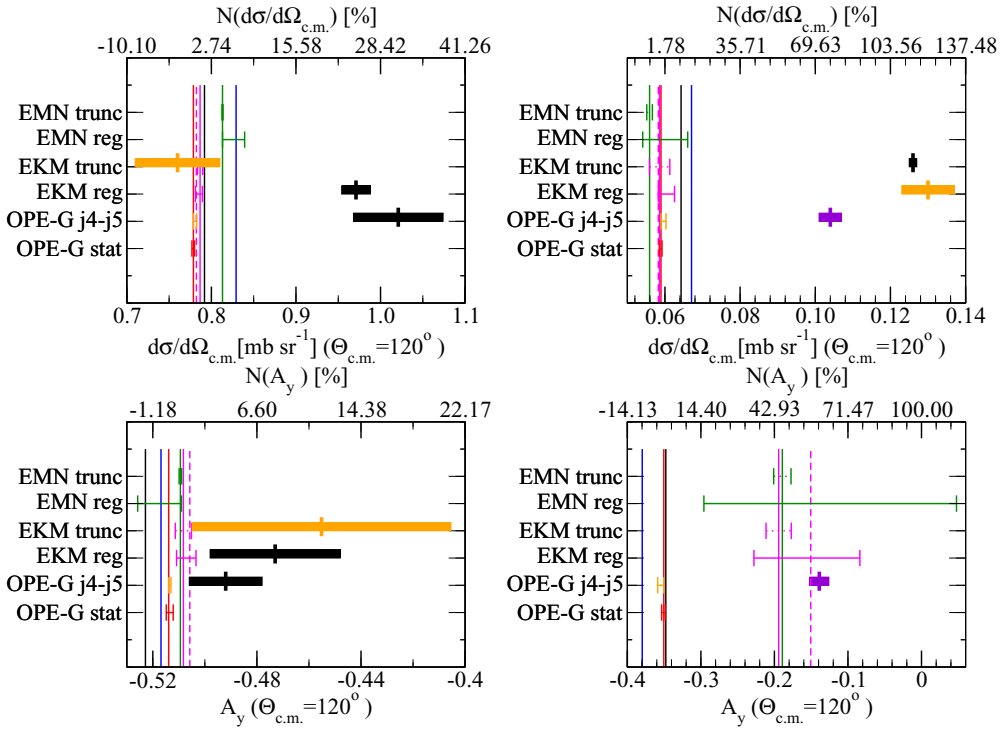

FIG. 15. The same as in Fig. 11 ($d\sigma/d\Omega$, the upper row) and Fig. 12 (A_y, the bottom row) at $\theta_{\text{c.m.}} = 120^\circ$ for $E = 65$ MeV (left) and $E = 200$ MeV (right) but supplemented by the experimental points at angles near $\theta_{\text{c.m.}} = 120^\circ$. Vertical and thin horizontal lines are as in Fig. 11, and filled rectangles represent experimental data and their statistical errors, as in Figs. 5 and 6.

multivariate probability distribution. Next, we investigated a distribution of our results and adopted one of estimators of their dispersion, $\frac{1}{2}\Delta_{68\%}$, as a measure of the theoretical statistical uncertainty. We also compared such statistical uncertainties for different observables with various types of theoretical errors, including the truncation errors and a dispersion due to using various models of the nuclear interaction. A comparison of uncertainties for the Nd elastic scattering cross section and a few polarization observables for the OPE-Gaussian model with other types of theoretical uncertainties leads to important conclusions about currently used models of $2N$ forces. First, all models of the NN interaction considered here deliver qualitatively and quantitatively similar predictions for the Nd elastic scattering observables. None of the interactions yields predictions systematically different from others and also no systematic grouping of predictions is observed. Second, we have found that in the case of the chiral forces, at small and medium energies, which are their natural domain of applicability, the dependence of predictions on the values of regulators dominates over other types of theoretical errors. At the highest investigated energy $E = 200$ MeV, which is at the limit of applicability of chiral forces, the truncation errors become important. It follows, that during a derivation of the chiral models, constant attention should be paid to the regularization methods applied. Current attempts to solve this problem result in a range of regulator parameters too broad to make the chiral forces such a precise tool in studies of nuclear reactions as desired and expected. It would be very interesting to check if this conclusion remains valid after taking into account also consistent $3N$ interaction at the order of chiral expansion investigated here (N^4LO).

Altogether, the presented results clearly show that modern nuclear experiments and theoretical approaches for the Nd scattering achieved similar precision. Having in mind that many investigations are currently focused on studying subtle details of underlying phenomena, there is a need to further improve precision both in theoretical as well as in experimental studies. From the theoretical side, continuous progress in deriving consistent NN and $3N$ forces from the χEFT gives hope that this goal will be achieved.

ACKNOWLEDGMENTS

We thank Dr. E. Ruiz Arriola and Dr. R. Navarro Pérez for sending us sets of parameters for the OPE-Gaussian model and for the valuable discussions. This work is a part of the LENPIC project and was supported by the Polish National Science Centre under Grants No. 2016/22/M/ST2/00173 and No. 2016/21/D/ST2/01120. The numerical calculations were partially performed on the supercomputer cluster of the JSC, Jülich, Germany.

[1] K. Sekiguchi, H. Witala, T. Akieda, D. Eto, H. Kon, Y. Wada, A. Watanabe, S. Chebotaryov, M. Dozono, J. Golak, H. Kamada, S. Kawakami, Y. Kubota, Y. Maeda, K. Miki, E. Milman, A. Ohkura, H. Sakai, S. Sakaguchi, N. Sakamoto, M. Sasano,

Y. Shindo, R. Skibinski, H. Suzuki, M. Tabata, T. Uesaka, T. Wakasa, K. Yako, T. Yamamoto, Y. Yanagisawa, and J. Yasuda, Phys. Rev. C **96**, 064001 (2017).
[2] G. J. Weisel, W. Tornow, A. S. Crowell, J. H. Esterline, G. M. Hale, C. R. Howell, P. D. O'Malley, J. R. Tompkins, and H. Witała, Phys. Rev. C **89**, 054001 (2014).
[3] B. von Przewoski *et al.*, Phys. Rev. C **74**, 064003 (2006).
[4] S. Kistryn, E. Stephan, A. Biegun, K. Bodek, A. Deltuva, E. Epelbaum, K. Ermisch, W. Glockle, J. Golak, N. Kalantar-Nayestanaki, H. Kamada, M. Kis, B. Klos, A. Kozela, J. Kuros-Zolnierczuk, M. Mahjour-Shafiei, U. G. Meissner, A. Micherdzinska, A. Nogga, P. U. Sauer, R. Skibinski, R. Sworst, H. Witala, J. Zejma, and W. Zipper, Phys. Rev. C **72**, 044006 (2005).
[5] C. R. Howell *et al.*, Few-Body Syst. **16**, 127 (1994).
[6] The Editors, Phys. Rev. A **83**, 040001 (2011).
[7] H. Witała, W. Glöckle, J. Golak, A. Nogga, H. Kamada, R. Skibiński, and J. Kuroś-Żołnierczuk, Phys. Rev. C **63**, 024007 (2001).
[8] A. Kievsky, M. Viviani, S. Rosati, D. Hüber, W. Glöckle, H. Kamada, H. Witała, and J. Golak, Phys. Rev. C **58**, 3085 (1998).
[9] T. Cornelius, W. Glockle, J. Haidenbauer, Y. Koike, W. Plessas, and H. Witała, Phys. Rev. C **41**, 2538 (1990).
[10] D. Hüber, W. Glockle, J. Golak, H. Witała, H. Kamada, A. Kievsky, S. Rosati, and M. Viviani, Phys. Rev. C **51**, 1100 (1995).
[11] J. L. Friar, B. F. Gibson, G. Berthold, W. Glöckle, T. Cornelius, H. Witała, J. Haidenbauer, Y. Koike, G. L. Payne, J. A. Tjon, and W. M. Kloet, Phys. Rev. C **42**, 1838 (1990).
[12] J. L. Friar, G. L. Payne, W. Glöckle, D. Hüber, and H. Witała, Phys. Rev. C **51**, 2356 (1995).
[13] E. Epelbaum, H. W. Hammer, and Ulf-G. Meißner, Rev. Mod. Phys. **81**, 1773 (2009).
[14] V. Bernard, E. Epelbaum, H. Krebs, and Ulf-G. Meißner, Phys. Rev. C **77**, 064004 (2008).
[15] V. Bernard, E. Epelbaum, H. Krebs, and Ulf-G. Meißner, Phys. Rev. C **84**, 054001 (2011).
[16] R. Machleidt and D. R. Entem, Phys. Rep. **503**, 1 (2011).
[17] D. R. Entem, R. Machleidt, and Y. Nosyk, Phys. Rev. C **96**, 024004 (2017).
[18] R. N. Perez, J. E. Amaro, and E. R. Arriola, Phys. Rev. C **88**, 064002 (2013).
[19] R. Navarro Pérez, J. E. Amaro, and E. Ruiz Arriola, Phys. Rev. C **89**, 064006 (2014).
[20] J. Dobaczewski *et al.*, J. Phys. G: Nucl. Part. Phys. **41**, 074001 (2014).
[21] D. G. Ireland and W. Nazarewicz, J. Phys. G: Nucl. Part. Phys. **42**, 030301 (2015).
[22] A. Ekström, G. Baardsen, C. Forssén, G. Hagen, M. Hjorth-Jensen, G. R. Jansen, R. Machleidt, W. Nazarewicz, T. Papenbrock, J. Sarich, and S. M. Wild, Phys. Rev. Lett. **110**, 192502 (2013).
[23] R. N. Perez, J. E. Amaro, and E. R. Arriola, Phys. Rev. C **91**, 054002 (2015).
[24] R. Navarro Pérez, J. E. Amaro, and E. Ruiz Arriola, J. Phys. G: Nucl. Part. Phys. **43**, 114001 (2016).
[25] P. Reinert, H. Krebs, and E. Epelbaum, Eur. Phys. J. A **54**, 86 (2018).
[26] R. J. Furnstahl, N. Klco, D. R. Phillips, and S. Wesolowski, Phys. Rev. C **92**, 024005 (2015).
[27] B. R. Barrett, P. Navratil, and J. P. Vary, Prog. Part. Nucl. Phys. **69**, 131 (2013).
[28] E. Epelbaum, H. Krebs, and Ulf-G. Meißner, Eur. Phys. J. A **51**, 26 (2015).
[29] S. Binder, A. Calci, E. Epelbaum, R. J. Furnstahl, J. Golak, K. Hebeler, H. Kamada, H. Krebs, J. Langhammer, S. Liebig, P. Maris, Ulf-G. Meißner, D. Minossi, A. Nogga, H. Potter, R. Roth, R. Skibiński, K. Topolnicki, J. P. Vary, and H. Witała, Phys. Rev. C **93**, 044002 (2016).
[30] R. Skibiński, J. Golak, K. Topolnicki, H. Witała, E. Epelbaum, H. Krebs, H. Kamada, Ulf-G. Meißner, and A. Nogga, Phys. Rev. C **93**, 064002 (2016).
[31] J. A. Melendez, S. Wesolowski, and R. J. Furnstahl, Phys. Rev. C **96**, 024003 (2017).
[32] E. Epelbaum, W. Glöckle, and Ulf-G. Meißner, Nucl. Phys. A **637**, 107 (1998); **671**, 295 (2000).
[33] E. Epelbaum, A. Nogga, W. Glockle, H. Kamada, Ulf-G. Meißner, and H. Witała, Phys. Rev. C **66**, 064001 (2002).
[34] D. R. Entem and R. Machleidt, Phys. Rev. C **68**, 041001(R) (2003).
[35] E. Marji, A. Canul, Q. MacPherson, R. Winzer, C. Zeoli, D. R. Entem, and R. Machleidt, Phys. Rev. C **88**, 054002 (2013).
[36] H. Witała, J. Golak, R. Skibiński, and K. Topolnicki, J. Phys. G: Nucl. Part. Phys. **41**, 094011 (2014).
[37] D. Rozpedzik, J. Golak, S. Kolling, E. Epelbaum, R. Skibinski, H. Witała, and H. Krebs, Phys. Rev. C **83**, 064004 (2011).
[38] R. Skibiński, J. Golak, D. Rozpędzik, K. Topolnicki, and H. Witała, Acta. Phys. Pol. B **46**, 159 (2015).
[39] E. Epelbaum, H. Krebs, and Ulf-G. Meißner, Phys. Rev. Lett. **115**, 122301 (2015).
[40] P. Maris *et al.*, EPJ Web Conf. **113**, 04015 (2016).
[41] S. Binder *et al.*, arXiv:1802.08584.
[42] R. Navarro Pérez, A. Nogga, J. E. Amaro, and E. Ruiz Arriola, J. Phys. Conf. Ser. **742**, 012001 (2016).
[43] R. B. Wiringa, V. G. J. Stoks, and R. Schiavilla, Phys. Rev. C **51**, 38 (1995).
[44] W. Glöckle *et al.*, Phys. Rep. **274**, 107 (1996).
[45] W. Glöckle, *The Quantum-Mechanical Few-Body Problem* (Springer-Verlag, Berlin, 1983).
[46] R. N. Perez, E. Garrido, J. E. Amaro, and E. Ruiz Arriola, Phys. Rev. C **90**, 047001 (2014).
[47] S. S. Shapiro and M. B. Wilk, Biometrika **52**, 591 (1965).
[48] H. Witała, W. Glöckle, D. Hüber, J. Golak, and H. Kamada, Phys. Rev. Lett. **81**, 1183 (1998).
[49] J. Kuroś-Żołnierczuk, H. Witała, J. Golak, H. Kamada, A. Nogga, R. Skibiński, and W. Glöckle, Phys. Rev. C **66**, 024003 (2002).
[50] S. Shimizu, K. Sagara, H. Nakamura, K. Maeda, T. Miwa, N. Nishimori, S. Ueno, T. Nakashima, and S. Morinobu, Phys. Rev. C **52**, 1193 (1995).
[51] H. Rühl *et al.*, Nucl. Phys. A **524**, 377 (1991).
[52] R. E. Adelberger and C. N. Brown, Phys. Rev. D **5**, 2139 (1972).
[53] G. Igo *et al.*, Nucl. Phys. A **195**, 33 (1972).
[54] K. Ermisch, H. R. Amir-Ahmadi, A. M. van den Berg, R. Castelijns, B. Davids, A. Deltuva, E. Epelbaum, W. Glockle, J. Golak, M. N. Harakeh, M. Hunyadi, M. A. de Huu, N. Kalantar-Nayestanaki, H. Kamada, M. Kis, M. Mahjour-Shafiei, A. Nogga, P. U. Sauer, R. Skibiński, H. Witała, and H. J. Wörtche, Phys. Rev. C **71**, 064004 (2005).

[55] J. Cub *et al.*, Few-Body Syst. **6**, 151 (1989).
[56] R. V. Cadman, J. Brack, W. J. Cummings, J. A. Fedchak, B. D. Fox, H. Gao, J. Golak, W. Glockle, C. Grosshauser, R. J. Holt, C. E. Jones, H. Kamada, E. R. Kinney, M. A. Miller, W. Nagengast, A. Nogga, B. R. Owen, K. Rith, F. Schmidt, E. C. Schulte, J. Sowinski, F. Sperisen, E. L. Thorsland, R. Tobey, J. Wilbert, and H. Witała, Phys. Rev. Lett. **86**, 967 (2001).
[57] S. P. Wells *et al.*, Nucl. Instrum. Methods Phys. Res., Sect. A **325**, 205 (1993).
[58] K. Topolnicki, J. Golak, R. Skibiński, and H. Witała, Phys. Rev. C **96**, 014611 (2017).